

Constructing 3D Virtual Reality Objects from 2D Images of Real Objects Using NURBS

Philippe Lavoie, Dan Ionescu, and Emil Petriu

University of Ottawa

School of Information Technology and Engineering
Ottawa, Ontario, Canada, K1N 6N5

Abstract—A new method for capturing and reconstructing 3D representations of real objects in a virtual reality system is introduced. Virtual reality applications allow users to navigate and interact with the 3D objects through the environment. This interaction requires that the 3D representation of real objects be highly accurate in modeling the reality. The novelty of the new methodology proposed, consists on the fact that it uses only a high resolution (7 megapixels or higher) digital camera and a projector in conjunction with 3D surface reconstruction techniques based on Non-Uniform Rational Bzier Spline (NURBS) functions. The 3D object reconstruction is based on finding unique control points on the 2D images of the object and constructing corresponding 2-D NURBS curves which contain the control points through a process of NURBS fitting. The control points are situated on grid lines which are extracted from the object surface on which a color coded grid is projected. The 2-D NURBS curves are projected into a 3-D space to eventually re-create the 3-D surface of interest. The method does not require any a priori knowledge of the absolute positioning or orientation of the camera and the projector as other 3D reconstruction techniques do. The precision of the method depends on the camera resolution and can attain easily sub-millimeters ranges. Examples illustrate the process.

Index Terms—Structured light, pseudo random coding, non-uniform rational Bzier Splines (NURBS), 3D NURBS approximation, 3D object reconstruction

I. INTRODUCTION

Present computing technologies allowed virtual reality (VR), augmented reality, and haptic applications to register tremendous progresses. A series of technical domains such as telecommunications, telelearning, medicine, etc use now VR techniques as exploratory means. VR technology became a natural extension of graphical user interfaces for various applications as it allows users to explore researched subjects in tangible and intuitive ways. The technical implications are manifold. Systems used for training in which the trainee uses a virtual reality object or environment to learn techniques related to his/her professional development, for ample simulation environments used to predict complex situations such as those implied by a natural disaster, or of the measures to devise in emergency situations created by humans or by industrial processes, and others are now available. In all the above the fidelity of reproducing the real object in a virtual environment is fundamental. As such, the capability of providing efficient and low cost systems to build avatars became a must in the VR domain.

The problem of recreating a 3-D views of an object from the information contained within two 2-D images is a subject

which received a great deal of attention from various researchers. A series of 3D reconstruction methods are recorded by the area literature. Each varies over the others in terms of precision, costs, computational requirements and advantages or in terms of what it can and cant be reconstructed. Barnard and Fischler [1] along with Dhond and Aggarwal [2] analyzed some of the methods used for stereo fusion. Jarvis [3], [4] wrote a perspective on range finding techniques such as structured lights, stereo fusion, focusing the cameras, camera motion, etc. Structured light is a well established technique to obtain three dimensional (3D) information of a scene obtained from recorded 2D images [3], [4]. Structured light methods use a specially designed light source to project sheets or beams of light with a known *a priori* spatial distribution onto the scene casting lines or points (dots) on the objects. The major advantage of this technique is that it circumvents the natural discontinuity/monotony properties of the object surfaces by replacing them with artificial features of structured light projections. These are better recovered and interpreted by computer vision. Salvi [5] wrote a report on the different codification strategies available in structured light systems. In this paper, a new system and methodology for 3D object reconstruction will be introduced. The system (as shown in Figure 4) consist of a projector, a digital camera, a rotating table, and a computer. The projector sends a structured light on the object placed on the rotating table. The scene is picked up by the digital camera and the information is processed by the computer using a specially designed application which generates a 3-D view. By repeating this process for a series of views the full object representation in a 3-D space is eventually recreated.

II. STRUCTURED LIGHT GRID ENCODED USING THE PSEUDO-RANDOM MULTI VARIATE SEQUENCE ALGORITHM

The structured light pattern used in the 3D reconstruction technique is created by using an extension of the Pseudo-random Binary Sequence (PRBS) [6] algorithm. Pseudo-random Multi Variate Sequences (PRMVS) [7] are generated by using Galois' theory applied to the problem of uniquely encoding a point in space.

A Galois field is the set of number $(0, 1, 2, \dots, N - 1)$ where N is prime and on which operations such as addition or multiplication are done using modulo N arithmetic. Fermat's

theorem states that any number n drawn from the Galois field set $(1, 2, \dots, N-1)$ has the following relationship $n^{N-1} = 1$. From the Fermat theorem, it is apparent that a number to an integral power is periodic with periodicity of $N - 1$:

$$n^{m+(N-1)} = n^m \times n^{(N-1)} = n^m$$

The property which enable a Galois field to create a PRMVS is that any Galois field always contains at least one number (α) called a generator (or primitive root). This generator has the property that the set of numbers $(\alpha^i | i = 0, \dots, N-2)$ is a permutation of the set $(1, 2, \dots, N-1)$. The sequence generated by the generator is periodic (from Fermat's theorem). So, for any integer (m), the set of numbers $(\alpha^i | i = m, \dots, m+N-2)$ is a permutation of the set $(1, 2, \dots, N-1)$.

The structured light pattern produced using PRMVS is a grid of coloured light lines such as magenta, red, green, yellow and cyan. This combination allows to generate a structured light grid with base 5 encoding. An example is shown in Figure 1 where each color was given a value: magenta (0), red (1), green (2), yellow (3) and cyan (4), the window size was set to 3 and the PRMVS was generated using the polynomial 3102 (expressed in base 5). This gives a sequence of 125 numbers over which a window of size 3 can slide without finding any repeating patterns.

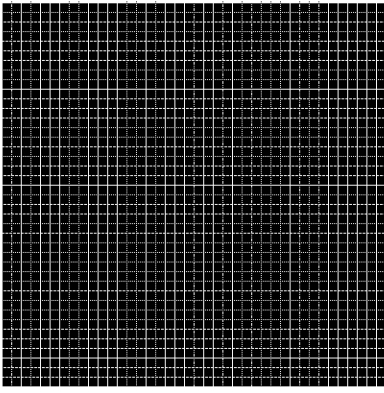


Fig. 1. A grid encoded with a PRMVS of base 5 and window length of 3.

The PRMVS is used to encode the X and Y axis. To retrieve a point on the structured light grid, one simply moves along the X axis until n data points are found, where n is the size of the viewing window. The same process is applied for the Y coordinate: one moves n data points along the Y axis to obtain the necessary information. With the information obtained, the data points are mapped into values and a table lookup is used to find the coordinate. It should be noted that points will not be labeled directly instead, lines will be labelled. A line will belong to the vertical or horizontal set of lines which constitute a $(X - Y)$ coordinate grid. This is useful as the reconstruction techniques is based on using special Beziers functions introduced in the next section.

III. NURBS - NON UNIFORM RATIONAL BÉZIER SPLINES

Non uniform rational Bézier splines (NURBS) have properties which are very useful for modeling a 3D object [8]:

- They offer a common mathematical form for representing analytic shapes (circles, conics, quadrics, etc.) and free-form curves and surfaces.
- They are invariant under affine transformations (scaling, rotation, translation and shear) and parallel and perspective projection.
- Their computation is reasonably fast and computationally stable.

NURBS are projection invariant which means that approximating the curve in 3D or its projection in 2D will yield the same curve. Since the present methodology uses 2D images extracting the object surfaces in 2D by obtaining the NURBS functions which best approximate it will result in the same precision when transposing the results in 3D. The technique precision depends therefore by the approximation accuracy of the NURBS function which increases with the number of points obtained from the 2D image. The latter is limited in this method only by the camera precision.

The mathematical definition of NURBS is captured by the following equations:

$$C(u) = \frac{\sum_{i=0}^n N_{i,p}(u) w_i P_i}{\sum_{i=0}^n N_{i,p}(u) w_i} \quad a \leq u \leq b \quad (1)$$

where P_i are the control points, w_i are the weights and $N_{i,p}$ are the B-spline basis functions defined on the non-periodic and nonuniform knot vector defined as

$$U = \underbrace{\{a, \dots, a\}}_{p+1}, u_{p+1}, \dots, u_{m-p+1}, \underbrace{b, \dots, b\}}_{p+1} \quad (2)$$

while the B-spline basis function of p -degree is defined using the recurrence definition as

$$\begin{aligned} N_{i,0}(u) &= \begin{cases} 1 & \text{if } u_i \leq u < u_{i+1} \\ 0 & \text{otherwise} \end{cases} \\ N_{i,p}(u) &= \frac{u - u_i}{u_{i+p} - u_i} N_{i,p-1}(u) + \\ &\quad \frac{u_{i+p+1} - u}{u_{i+p+1} - u_{i+1}} N_{i+1,p-1}(u) \end{aligned} \quad (3)$$

Homogeneous coordinates can represent a rational curve in n dimensions as a polynomial curve of $n + 1$ dimensions. The homogeneous control points are written as $P_i^w = (w_i x_i, w_i y_i, w_i z_i, w_i)$ in a four dimensional space where $w \neq 0$. To obtain P_i , we divide all the coordinates by the fourth coordinate w . This operation corresponds to a perspective map with the center at the origin. With these coordinates, the NURBS curve can be redefined as

$$C^w(u) = \sum_{i=0}^n N_{i,p}(u) P_i^w \quad (4)$$

IV. EXTRACTING NECESSARY FEATURES FOR FITTING NURBS

A. Intersection Point Extraction

The precision of the 3-D reconstruction relies on the algorithms used for point extraction and edge detection. The zero-crossing edge detectors were chosen as they can be extended to sub-pixel accuracy. A pixel is marked as an edge pixel, if in its

immediate area there is a zero crossing having negative slope of the second directional derivative taken in the direction of the gradient [9]. The directional derivative can be computed from the knowledge of the directional derivative D_1 and D_2 . The gradient magnitude is computed as $\sqrt{D_1^2 + D_2^2}$ and its direction as $\arctan(D_2/D_1)$. With the integrated directional derivative gradient edge detector operator it is possible to compute the edge location with subpixel accuracy. It has been shown [10] that for a step edge the quadratic fitting yields the proper result.

B. Line Detection Algorithm

Once edge points are found, the system still needs to interpret the edge data and group it into lines. The algorithm used for the above operation is applied to the horizontal edge points to create a list of horizontal lines, and to the vertical edge points to generate a list of vertical lines.

The use of lines instead of points in this methodology, is related to the obvious fact that a line is a continuous of points, which allows calculating the proper NURBS function with a very high precision.

The use of the edge line instead of the center line improves the accuracy of the 3-D reconstruction process. One of the premises for illuminating an object with a line is that the illumination creates a plane of light in 3-D. The object intersects this plane. That premise is changed by the use of the two edge lines instead of a single line. It implies that two planes instead of one plane are projected for each grid line.

V. NURBS CURVE AND SURFACE FITTING

Once the list of points which compose a line is known, a NURBS curve is looked for to fit those points. The point of interest is simply the intersection of the vertical and the horizontal NURBS curve. NURBS curve fitting goes through the set of points and has at least the same number of control points than the number of points to be fitted.

The procedure of NURBS curve fitting presented in this paper uses an approximation technique as it is considered better than the global interpolation, and the least square fitting techniques. When using the approximation technique, the number of control points that will be used to fit through the set $\{U_k\}$ of points is not known in advance. The curve will be fitted to satisfy a minimizing function, i.e. reduce the distance between the curve and the points to be fitted. Despite that it is more difficult than least squares fitting it yields to visually correct results within an error tolerance E .

The approximation methods are iterative and rely on the degree of elevation and knot reduction to perform the fitting. The general knot reduction algorithm is as follows. Let u_r be an interior knot of a p th degree non-rational curve $C(u)$ where $u_r \neq u_{r+1}$, and the multiplicity of u_r is s . Let $\hat{C}(u)$ denote the curve obtained by removing one occurrence of u_r . The new control points P_i^1 and P_j^1 are computed from the left and

the right.

$$P_i^1 = \frac{P_i^0 - (1 - \alpha_i)P_{i-1}^1}{\alpha_i}$$

where $r - p \leq i \leq \frac{1}{2}(2r - p - s - 1)$

$$P_j^1 = \frac{P_j^0 - \alpha_j P_{j+1}^1}{(1 - \alpha_j)}$$

where $\frac{1}{2}(2r - p - s + 2) \leq j \leq r - s$ (5)

with

$$\alpha_k = \frac{u - u_k}{u_{k+p+1} - u_k} \quad k = i, j$$

VI. TSAI'S CAMERA MODEL

The camera model is important for the precision of the 3D object reconstruction technique. Tsai [11] has created a camera model which is very efficient for camera calibration and thus for the control of the accuracy of 3D object reconstruction process. In [12] the Tsai model is used in conjunction with a similar structured light grid to automatically find the camera and projector parameters needed to calculate with a given precision the 3D surfaces which describe the computer three dimensional image of a given real object.

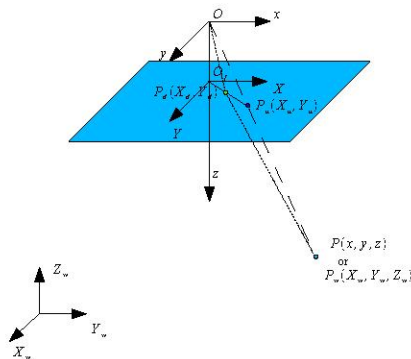


Fig. 2. The camera model proposed by Tsai. This model accounts for radial lens distortion.

The model is the famous pinhole model with the radial lens distortion taken into account [11]. The model is depicted in Figure 2. The following notation is used inside that figure:

- $P_w(X_w, Y_w, Z_w) \in \mathbb{R}^3$ is the 3-D world coordinate of the object point P .
- $P(x, y, z) \in \mathbb{R}^3$ is the point P in the 3-D camera coordinate system.
- $O \in \mathbb{R}^3$ is the origin of the 3-D camera coordinate system.
- z axis is the z axis of the camera coordinate system, which is the same as the optical axis.
- $(X, Y) \in \mathbb{R}^2$ is the image coordinate system centered at O . It is the intersection of the optical axis z and the front image plane. It is parallel to the x and y axes.
- $O_f \in \mathbb{R}$ is the focal distance between the front image plane and the optical center O .

- $(X_u, Y_u) \in \mathbb{R}^2$ is the image coordinate of the point $P(x, y, z)$ if a perfect pinhole camera is used.
- $(X_d, Y_d) \in \mathbb{R}^2$ is the actual image coordinate of the point $P(x, y, z)$. It differs from (X_u, Y_u) due to lens distortion.
- $(X_f, Y_f) \in \mathbb{R}^2$ is the pixel location of the point (X_d, Y_d) . This point is not shown in the graphic. The origins for the pixels are not centered on the image, but are usually at the lower left corner of the image.

There are two kinds of distortion: radial and tangential. For each kind of distortion an infinite series is required. However, Tsai's experience shows that for industrial machine vision application, only radial distortion needs to be considered, and only one term is needed from the series. Any more elaborate modeling not only would not help but also would cause numerical instability in the calibration process.

The calibration process described by Tsai uses non linear search techniques to find values for most of the parameters. Some values, like the number of pixels, have to be provided.

The projector model follows the same model and its equations are an adapted copy of the camera model.

VII. BACK PROJECTION OF AN IMAGE POINT

Given a point $P_f = (X_f, Y_f)$ in the image frame buffer, it is possible to back project this point into a 3-D world coordinate system. This creates a line in 3-D. Fixing the value for Z yields a point in the 3-D world coordinate system.

The back projection algorithm projects an image point into the 3-D world coordinate system. The input of the algorithm are the coordinates of the image point inside the frame buffer (X_f, Y_f) and the desired P_z value in the world coordinate system. The steps are

STEP 1 Compute the real image coordinate (X_d, Y_d) from the pixel in frame memory (X_f, Y_f) .

$$X_d = \frac{X_f - C_x}{s_x d_x^{-1}} \quad (6a)$$

$$Y_d = \frac{Y_f - C_y}{d_y^{-1}} \quad (6b)$$

STEP 2 Compute the radial distortion (D_x, D_y)

$$D_x = X_d(\kappa_1 r^2) \quad (7a)$$

$$D_y = Y_d(\kappa_1 r^2) \quad (7b)$$

$$r = \sqrt{X_d^2 + Y_d^2} \quad (7c)$$

STEP 3 Compute the undistorted point (X_u, Y_u)

$$X_u = X_d + D_x \quad (8a)$$

$$Y_u = Y_d + D_y \quad (8b)$$

STEP 4 The inverse of the projection is used to compute the values for P_x and P_y by using Equation ??.

The camera model makes it clear that if the only information known about a point is its location (X_f, Y_f) in pixels, then

(after calibration) the only information which can be obtained about its location in the 3-D world coordinates is the 3-D "line" in which it lies. Actually, it is not even a line as a pixel is not an infinitely small point but a square of a finite size. This aspect is minimized for the camera model and is helpful for the projector model.

The 3-D reconstruction process is thus as follows:

- 1) For an horizontal NURBS curve C_i , the corresponding horizontal grid line j from the projector is used to create a 3-D world coordinate surface.

The calibration process takes into account the radial distortion of the projector. The radial distortion implies that, in a perfect world, a plane of light would be created by the projection of a line through space.

A NURBS curve can be used to represent a conic or in the case of radial distortion a parabolic curve. Let P_0 and P_2 be the end points of the conic arc, let T_0 and T_2 be the derivative of the arc at those end points and let P be an arbitrary point on the parabolic curve. Then, it is possible to create a NURBS curve which corresponds to this parabolic curve. The control points P_0 and P_2 are already defined and the point P_1 is obtained by intersecting the line $[P_0, T_0]$ and $[P_2, T_2]$. The weights w_0 and w_2 are both set to 1. The only unknown is w_1 which can be solved for using geometric arguments (see [13]). This method yields the following equation for w_1 :

$$w_1 = \frac{(1-u)^2(P - P_0) \cdot (P_1 - P)}{2u(1-u)|P_1 - P|^2} + \frac{u^2(P - P_2) \cdot (P_1 - P)}{2u(1-u)|P_1 - P|^2} \quad (9)$$

where

$$u = \frac{a}{1+a} \quad a = \sqrt{\frac{|P_0Q|}{|QP_2|}} \quad (10)$$

and Q is the projection of P onto the line $[P_0, P_2]$ using P_1 as a center of projection.

To create the surface of projection of this line onto space the ruled surface algorithm is used. The ruled surface algorithm requires two curves and it is the same algorithm as skinning [14] applied to only two curves. The second curves is obtained by projecting the curve obtained above onto space the projection must be done far enough to cover the object being illuminated. The projection equations are the same as the ones for step 2 of the reconstruction algorithm. The ruled surface is then simply defined as $U = \{0, 0, 0, 1, 1, 1\}$, $V = \{0, 0, 0, 1, 1\}$, $W_j^i = w_i^1 R_i^1 = P_i^1$ and $R_i^2 = P_i^2$.

Intersecting a line with a NURBS surface is done using a Newton iterative method to compute the intersection point. The method uses the geometrical properties of a NURBS surface and its control net to limit the search space.

- 2) The 3-D world coordinate NURBS curve is created by using the same knot vector as C_i and the control point set defined by P'_j .

3) The process is repeated for every horizontal line.

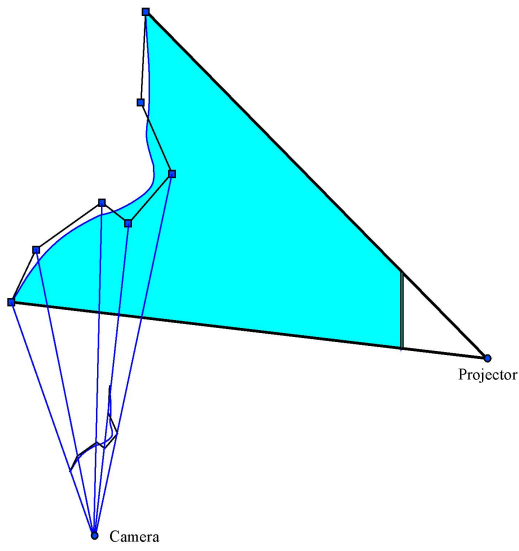


Fig. 3. The 3-D reconstruction process.

The new NURBS curve is now in 3-D world coordinates.

Creating a surface which represents the object is done by the interpolation of a bidirectional curve network.

VIII. EXAMPLES OF RECONSTRUCTED OBJECTS

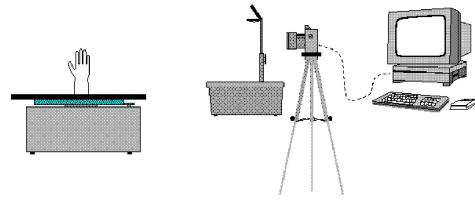
In this section the system and the technique of building a 3D image of a real object introduced in this paper, is described. The section also presents some results obtained. The system shown in Figure 4 is used to capture a complete set of 2D images of the object to be used in a VR environment.

A series of objects were used to verify the system and methodology process and accuracy. In what follows some of these object 3D reconstructions steps will be shown.

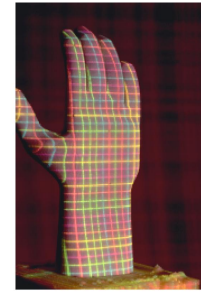
1) The Utah teapot: The structured light is projected on the famous Utah teapot [15] as shown in Figure 5. This object has a complex topology, it self-shadows, has hidden surface issues and both convex and concave surfaces. The Utah teapot is defined with B-splines patches. This simplifies the process of analyzing the error between the known Utah teapot and the surface generated with the methodology proposed for 3-D reconstruction. Using calibrated parameters, the 3-D lines are projected into 3-D space to create a view of the object. This view is limited to the grid lines which have sufficient lighting conditions.

The data to generate a raytracing of the Utah teapot is a set of B-splines patches. This set of B-spline patches can be compared with the set of NURBS surfaces generated by the methodology presented in thesis in order to compute the error in 3-D reconstruction. The results obtained with various stages of the methodology are shown in Table VIII-1.

The error between the Utah teapot and a NURBS curve or NURBS surface is the distance between a point on the NURBS curve or surface and the point on the Utah teapot that is closest to it.

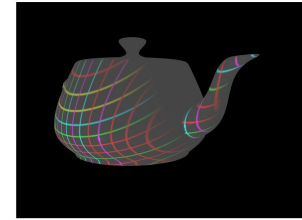


(a)

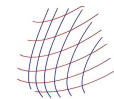


(b)

Fig. 4. a) The setup for the 3-D reconstruction of an object. b) A captured image from that setup.



(a)



(b)

Fig. 5. (a) The Utah teapot illuminated by the structured light. (b) The 2-D lines detected by the methodology.

Object	Mean (mm)	Std Dev (mm)
Horizontal Grid Lines	0.110745	0.0986030
Vertical Grid Lines	0.0538629	0.025974
Horizontal Skin Surface	0.0940525	0.0792902
Vertical Skin Surface	0.121947	0.0884404
Gordon Surface	0.0305820	0.0391224

Object	Min (mm)	Max (mm)
Horizontal Grid Lines	0.00179233	0.465082
Vertical Grid Lines	0.00384417	0.110581
Horizontal Skin Surface	0.000346476	0.558296
Vertical Skin Surface	0.000663184	0.449805
Gordon Surface	0.0000217415	1.05252

TABLE I

ACCURACY WITH THE UTAH TEAPOT.

The Table VIII-1 shows results for the vertical and horizontal grid lines projected in the 3-D world coordinate system. It also shows the errors when skinning is used from the vertical lines or the horizontal lines. Finally, the error obtained when using the Gordon surface is also shown.

The error between a NURBS surface and the Utah teapot is computed by taking 100 samples across that surface and then finding the closest distance between those samples and the Utah teapot surface. The error for that sample is the average of these closest distances.

The maximum error obtained with the Gordon surface generated is localized to a single surface patch and not to the entire set of surfaces that are required to cover the surface. The average error obtained with the Gordon surface is smaller than the one obtained with simply the grid lines. It should be noted that although the vertical and horizontal lines projection do not match perfectly, the algorithm introduced in this paper accounts for this and allows the system to obtain a better surface representation.

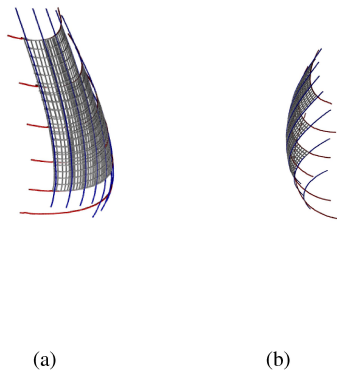


Fig. 6. Generated views of the Utah teapot. The view in (a) is from the left and the view in (b) is from the right of the object.

2) The Cow Butter Holder: This object is a butter holder in the shape of a cow (see Figure 7). Like the teapot object, it is made of white ceramic and it reflects light in a similar manner. It is relatively smooth. Figure 7(b) shows the results obtained by the 3D reconstruction process proposed in this paper for the Cow Butter Holder.

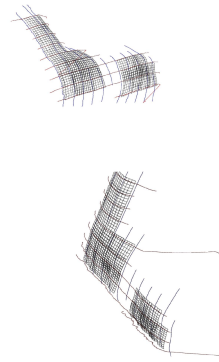
3) The Tea Cup: The tea cup is made from white ceramic. The bottom of it is smooth and the top part contains some flower patterns in 3-D. The flower pattern lies between grid lines (see Figure 8) and only the sections that are on a grid line are affecting the 3-D surface generation. The results are shown in Figure 8(b).

4) The Milk Holder: The milk holder is also made from white ceramic as shown in Figure 9. It is a smooth 3-D surface except near the beak where there is a smooth edge. The smooth edge is properly captured by the algorithm and to illustrate this, a section of the image is zoomed and its corresponding 3-D representation is shown in Figure 10(a).

5) The SLA Hand Object: The hand object is made by a stereo lithography (SLA) system. It is a non reflective surface



(a) Input image



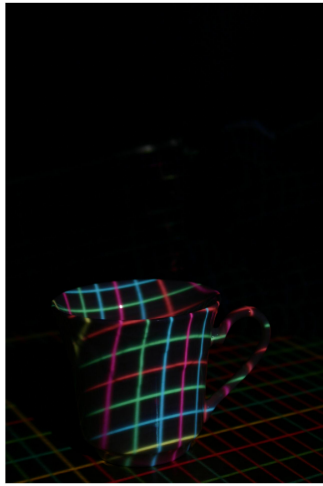
(b) Generated surface from two different view points.

Fig. 7. Input image and the 3-D representation of the cow butter holder object.

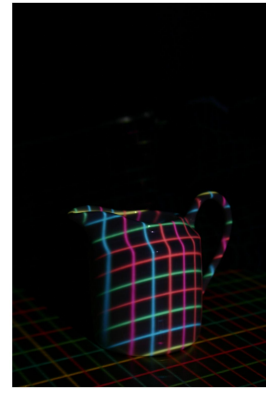
that slightly absorbs the light. The system is able to capture properly all the contiguous areas found on the hand object as it is apparent in Figure 11. The thumb area is also properly captured by the NURBS curves, however due to the angle of the projector a discontinuity is created that prevents the system from having a contiguous area for a surface reconstruction near that part of the hand.

IX. CONCLUSION

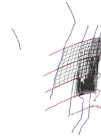
The paper focussed and discussed the design of a system and the techniques used by this system to reconstruct the 3D image of a real object with a desired high accuracy in a very low budget constraint. The novelty of the technique consists in the following contributions. First it is using only one digital camera and a projector, which allows users to direct the heavy expenditures towards a very good digital camera. The projector is used to project a specially designed structured light pattern, in a form of grid, on the rotating object. The randomness of the grid pattern uniquely locates points on the object surface. This technique resolves what other reconstruction techniques recognize it as a very difficult part of the 3D reconstruction process. It uniquely locates and orients a point on any type of object surfaces especially the flat and texture-less ones. The problem of calibrating the camera and also the projector is considered complex enough to be left for yet another paper related to this subject.



(a) The input image



(a) Input image

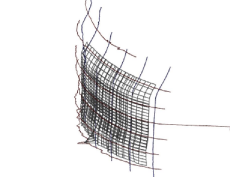
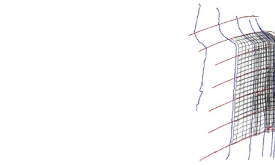


(b) The generated surface from two different view points.

Fig. 8. Input image and the 3-D representation of the tea cup object.

REFERENCES

- [1] S. T. Barnard and M. A. Fischler, "Computational stereo," *ACM Computing Surveys*, vol. vol. 14, pp. pages 553–572, Dec. 1982.
- [2] U. R. Dhond and J. Aggarwal, "Structure from stereo — a review," *IEEE Trans. on Systems, Man and Cyber.*, vol. vol. 19, pp. pages 1489–1510, Nov./Dec. 1989.
- [3] R. A. Jarvis, "A perspective on range finding techniques for computer vision," *IEEE Trans. Pattern anal. Machine Intel.*, vol. vol. 5, pp. pages 122–139, March 1983.
- [4] P. Will and K. Pennington, "Grid coding: A preprocessing technique for robot and machine vision," in *Proc. 2nd Int. Joint Conf. Artificial Intell.*, pp. 66–68, Sep. 1971.
- [5] E. Mouaddib, J. Batlle, and J. Salvi, "Recent progress in structured light in order to solve the correspondence problem in stereovision," in *Proceedings of the 1997 IEEE International Conference on Robotics and Automation*, (Albuquerque, New Mexico), April.
- [6] P. Vuytske and A. Oosternlink, "Range image acquisition with a single binary encoded light pattern," *IEEE Trans. Pattern anal. Machine Intel.*, vol. vol. 12, pp. pages 148–164, Feb. 1990.
- [7] P. Lavoie, D. Ionescu, and E. M. Petriu, "3-d object reconstruction

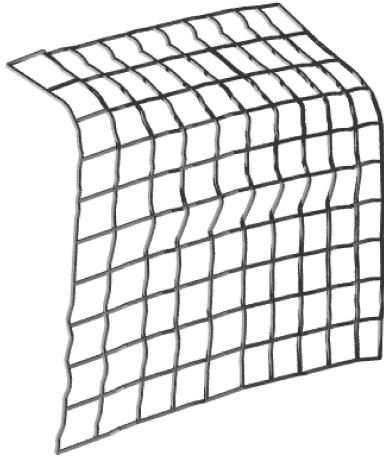


(b) Generated surface from two different view points.

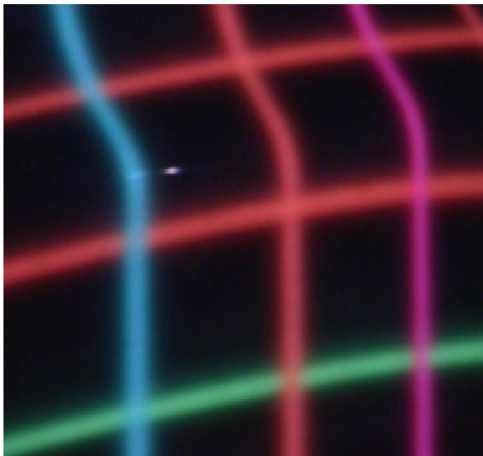
Fig. 9. Input image and the 3-D representation of the milk holder object.

using color coded grids and nurbs," in *Proceedings ET&VS-IM/97 IEEE Workshop on Emergent Technologies and Virtual Systems for Instrumentation Measurement*, (Niagara Falls, Canada), pp. 99–104, 1997.

- [8] L. Piegl, "On nurbs: A survey," *EEE Computer Graphics and Applications*, vol. vol. 10, no. no. 1, pp. pages 55–71, 1991.
- [9] R. M. Haralick, "Zero-crossing of second directional derivative edge operator," in *SPIE symposium on robotic vision*, p. 23 pages, 1982.
- [10] F. Devernay, "A non-maxima suppression method for edge detection with sub-pixel accuracy," Tech. Rep. no. 2724, Institut National de Recherche en Informatique et en Automatique, November 1995.
- [11] R. Y. Tsai, "A versatile camera calibration technique for high-accuracy 3d machine vision metrology using off-the-shelf tv cameras and lenses," *IEEE Journal of Robotics and Automation*, vol. vol. 3, pp. pages 323–344, 1987.
- [12] P. Lavoie, D. Ionescu, and E. Petriu, "Camera and projector calibration with nurbs..," Submitted to *IEEE Transactions on Instrumentation and Measurements*, 2007.
- [13] L. Piegl, "A technique for smoothing scattered data with conic sections," *Computers in Industry*, vol. vol. 9, pp. pages 223–237, 1987.



(a) 3-D NURBS Surface



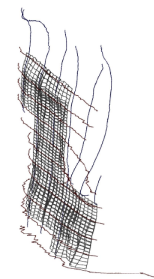
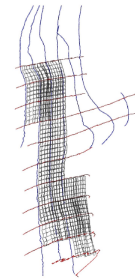
(b) Section of the input image.

Fig. 10. Generation of a 3-D surface near the edge.

- [14] P. Lavoie, *3D object reconstruction using structured light and two 2D images*. PhD thesis, University of Ottawa, November 2004.
- [15] S. Baker, "A brief history of the utah teapot," Tech. Rep. RR-1984, Steve Baker, April 1999.



(a) Input image



(b) Generated surface from two different view points.

Fig. 11. Input image and the 3-D representation of the hand object.